FES Joint Facilities Research Milestone 2010

Annual Target: Conduct experiments on major fusion facilities to improve understanding of the heat transport in the tokamak scrape-off layer (SOL) plasma, strengthening the basis for projecting divertor conditions in ITER. The divertor heat flux profiles and plasma characteristics in the tokamak scrape-off layer will be measured in multiple devices to investigate the underlying thermal transport processes. The unique characteristics of C-Mod, DIII-D, and NSTX will enable collection of data over a broad range of SOL and divertor parameters (e.g., collisionality ν^*, beta β, parallel heat flux $q_{||}$, and divertor geometry). Coordinated experiments using common analysis methods will generate a data set that will be compared with theory and simulation.

Quarter 2 Milestone

Initial planned experiments will have been carried out on at least one of the three facilities.

Completion of 2nd Quarter Milestone

The targeted goal for the second quarter was achieved, as documented in the remainder of this report. To be specific, new experiments were conducted in Alcator C-Mod and DIII-D, including a joint dimensionless similarity experiment between the two devices. Activities in NSTX centered about refining analysis of previous data, and diagnostic preparation for the next set of experiments that will commence in the 3rd quarter FY10. The progress at each facility is described in the following sections.

Alcator C-Mod research (B. LaBombard, J. Terry)

Two Alcator C-Mod mini-proposals have been developed to support the FY10 joint facilites research on boundary layer heat transport, focusing on L-mode and H-mode plasmas. These proposals may be accessed through the following links:

MP#570, "Boundary layer heat transport experiments in L-mode plasmas"

MP#591, "Boundary layer heat transport experiments in H-mode plasmas"

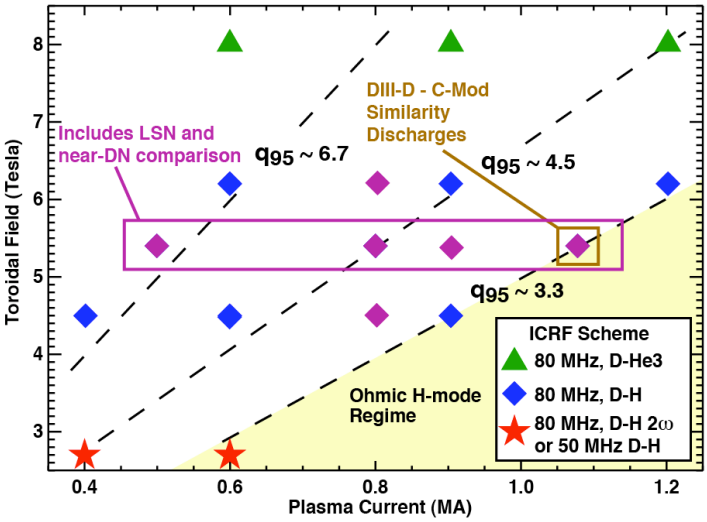

Figure 1. Plasma current and toroidal field combinations to be investigated for boundary layer heat flux experiments. ICRF power scans are to be performed at each combination. Plasma density will be chosen so as to produce stationary H-modes.

These aggressive proposals, calling for significant blocks of run time, are slated to span the two planned C-Mod run campaigns for FY10. In preparation for the joint experiments, MP#570 received some preliminary run time during the FY09 period, mostly for diagnostic commissioning in L-mode discharges. The plan for MP#591, which focuses on H-mode discharges, was developed in close consultation with DIII-D and NSTX. EDA H-mode plasmas were selected for study, since they are steady-state and cover the largest operational-space available in C-Mod.

Both mini-proposals include detailed plans for measuring the divertor heat flux 'footprints' and their mappings to the heat flux channel widths at the outer midplane in a variety of plasma conditions. The proposed parameter space for H-mode discharges is indicated in Fig. 1, which also highlights the exploration of 'dimensionless similarity discharges' that attempt to match shape and dimensionless plasma physics parameters (ν^*, ρ^*, β) in the pedestal region with DIII-D discharges. In addition to these parameter scans, the effect of magnetic connection length on power e-folding widths is to be explored by comparing lower single null versus near double null discharges under otherwise identical conditions. This will help to differentiate among the roles of plasma

current, safety factor and connection length in empirical scalings. Results from these studies will be presented at the 2010 Plasma-Surface Interactions conference and will be published subsequently[1, 2]. In all of these experiments, turbulence imaging diagnostics are to be employed to follow systematic trends in the fluctuation spectra from the plasma edge and SOL.

At the present time, five run days have been executed for H-mode boundary layer heat flux experiments (MP#591). All of the target discharges represented by the purple symbols in Fig. 1 have been successfully produced, including the C-Mod/DIII-D similarity discharges. A summary of those parameter scans is:

- B_t=5.4T: I_p=0.5, 0.8, 0.9, 1.0 MA with auxiliary power scan
- B_t=6.2T: I_p=0.8 MA with auxiliary power scan
- B_t=4.5T: I_p=0.8 MA with auxiliary power scan
- DIII-D similarity discharge with B_t=5.4T, I_p=0.9 MA, P_{aux} scanned from 1 to 4 MW

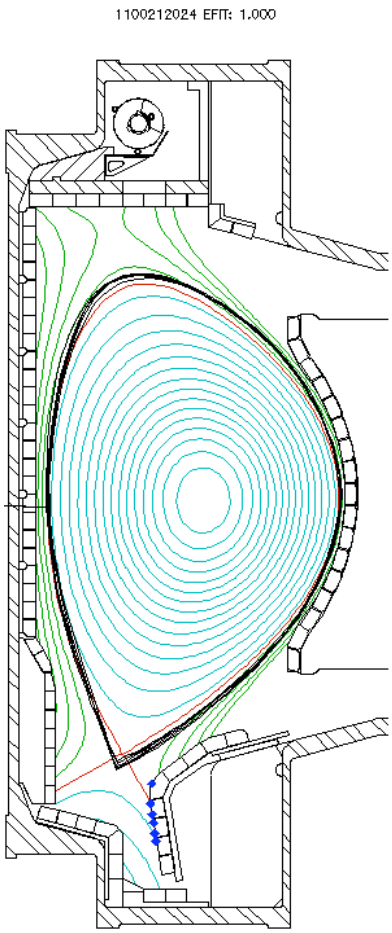

Figure 2. Cross section of C-Mod flux surfaces (LCFS in red) overlaid with LCFS of DIII-D's similarity discharge (in black)

A good plasma boundary shape match has been obtained between C-Mod and DIII-D for the similarity discharge set (Fig. 2). This shape will also be produced in NSTX. Stable EDA H-modes were obtained at I_p=0.9 MA during the initial run day, slightly below the target current of 1.0 MA. Data from EDA H-modes at 1.0 MA were obtained in a follow-up run. The auxiliary ICRF heating power was varied between 1 and 4 MW, with fixed and swept strike point and a variety of pedestal profiles were obtained. For all of the purple parameter-space-points in Fig. 1, divertor surface temperature profiles have been measured, as have electron temperature and density profiles at the outboard midplane.

An example of one such measurement is illustrated in Fig. 3. Plasma current, density and power time histories are shown in the top panel, where the EDA H-mode is produced from 0.9-1.55s and P_{SOL}~2-3 MW. A sub-image of the surface temperature on the instrumented and toroidally ramped divertor target tiles is shown in panel (b). A plot of a fitted profile of the surface temperature at a small slice of toroidal angle as a function of poloidal distance up the target surface is shown in panel (c). The same profile is shown plotted vs ρ mapped to the outboard midplane in panel (d). These surface temperature time histories will be input to a 2D finite-element heat-transport model of the outer divertor target plate structure (presently under development) in order to infer the heat flux 'footprint' profiles as plasma parameters are varied. The IR thermography results, with emphasis on the areas where the measurement difficulties are similar to those expected

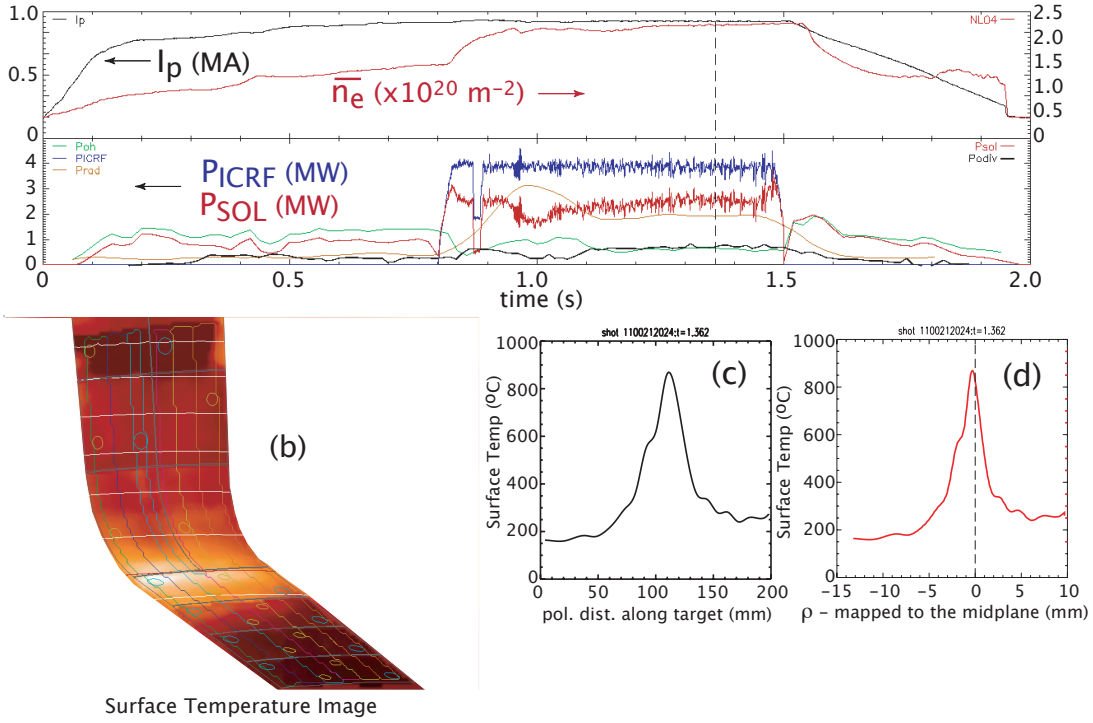

Figure 3. Plasma parameters and IR thermography results from a 0.9 MA, 5.4T EDA H-mode discharge. (a) Plasma parameter time traces. (b) A sub-image of the IR camera's view of the instrumented and toroidally ramped divertor section for which the color scale is the log of the surface temperature. Overlaid: in blue, green, yellow - the outlines of the instrumented tiles and locations of the thermocouples, etc.; in red – the strike point; in white - flux surfaces in 2 mm (mapped to midplane) increments. (c) T_{surf} profile vs poloidal distance along the target surface at a fixed toroidal angle. (dist=0 at the bottom of the shaped divertor and the bottom of the sub-image.) (d) T_{surf} profile vs ρ mapped to the midplane.

for ITER, will be presented at the 2010 High Temperature Plasma Diagnostics Conference[3].

C-Mod is scheduled for an in-vessel opening/access to begin in April 2010. During this time the present instrumented divertor section will be replaced and refurbished with new probes, thermocouples and calorimeters. When the 2010 run campaign resumes, multiple run days are anticipated for JRT milestone experiments, with a roughly equal division between L-mode (MP#570) and H-mode discharge (MP#591) explorations.

DIII-D research (C. Lasnier)

In DIII-D, a boundary joint facility similarity experiment was carried out on March 9 and 11, with the goal of measuring heat flux under similar conditions in DIII-D, C-Mod, and NSTX. Rajesh Maingi traveled to DIII-D to participate. The C-Mod team provided profiles from C-Mod that were compared with DIII-D profiles during the day.

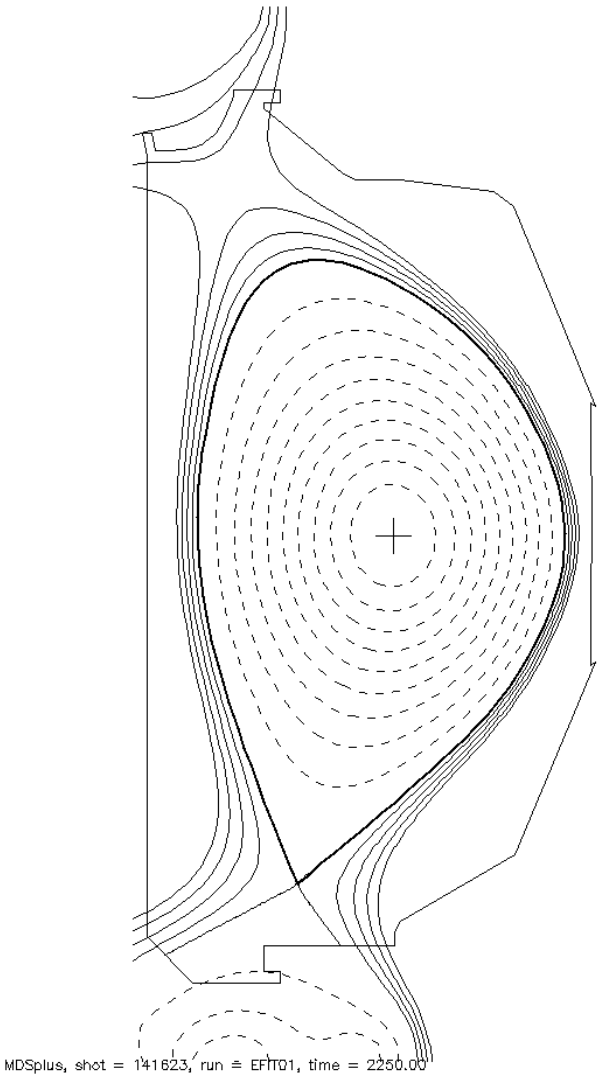

Figure 4. DIII-D equilibrium for the joint experiments. Compare with Fig. 2 in the C-Mod section

The magnetic equilibrium shape was reproduced from pedestal similarity experiments performed with C-Mod in 2001, which is similar to a shape that C-Mod and NSTX can run (the same elongation, triangularity, and

squareness) (see Figure 4).

The first part of the day used gyrotrons and no beams, to better compare heat flux with C-Mod RF-heated discharges. The second part used neutral beams de-rated to 43 kV from the normal 80 kV accelerating voltage, and no gyrotrons. We scanned power levels in two steps per shot: 1,2,3,4,5, and 6 gyrotrons, fixed power with varying plasma current, and at two toroidal field values. The gyrotron power levels were repeated using beams running at 43 kV. We obtained lower divertor IR camera data at two toroidal locations separated by 105 degrees, data from plunging Langmuir probes at the midplane and divertor, floor Langmuir probes, fluctuation reflectometry, and beam emission spectroscopy during the beam shots, as well as numerous other diagnostic measurements. An outer strike point heat flux radial profile is shown in Fig. 5. The private flux region is on the left.

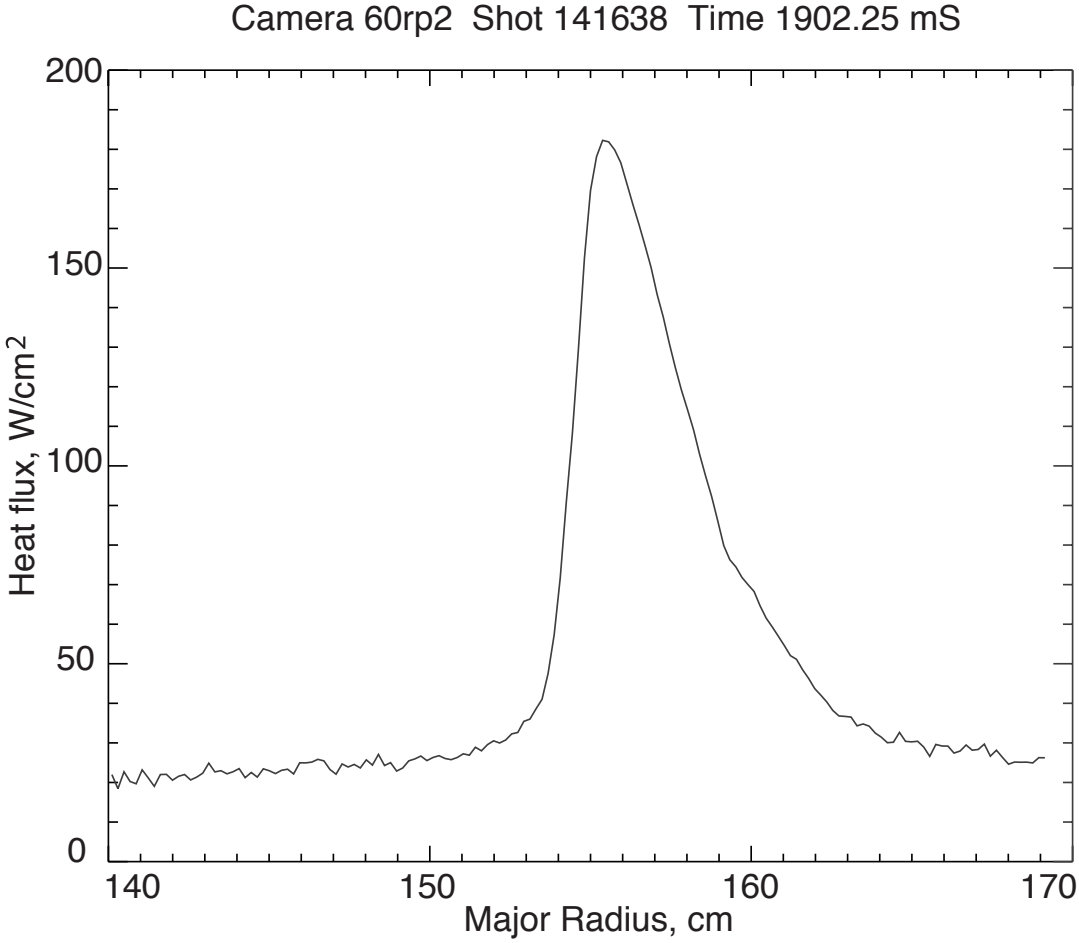

Fig. 5. Outer strike point heat flux radial profile

The data obtained in these discharges will serve as the large major radius part of the size scaling between DIII-D and C-Mod. The DIII-D data will be analyzed to determine the width of the divertor target heat flux mapped back to the outboard midplane, specified as a fraction of the minor radius. The Thomson scattering upstream data will also be analyzed to specify the pedestal and separatrix values of beta, collisionality and ion gyro-radius. A recent experiment in C-Mod attempted to match these upstream dimensionless parameters while measuring the divertor target heat flux profile. The relationship of the heat flux width in DIII-D to C-Mod for similar upstream dimensionless parameters will be used to examine the size scaling of the divertor heat flux profile from current devices to future burning plasma tokamaks.

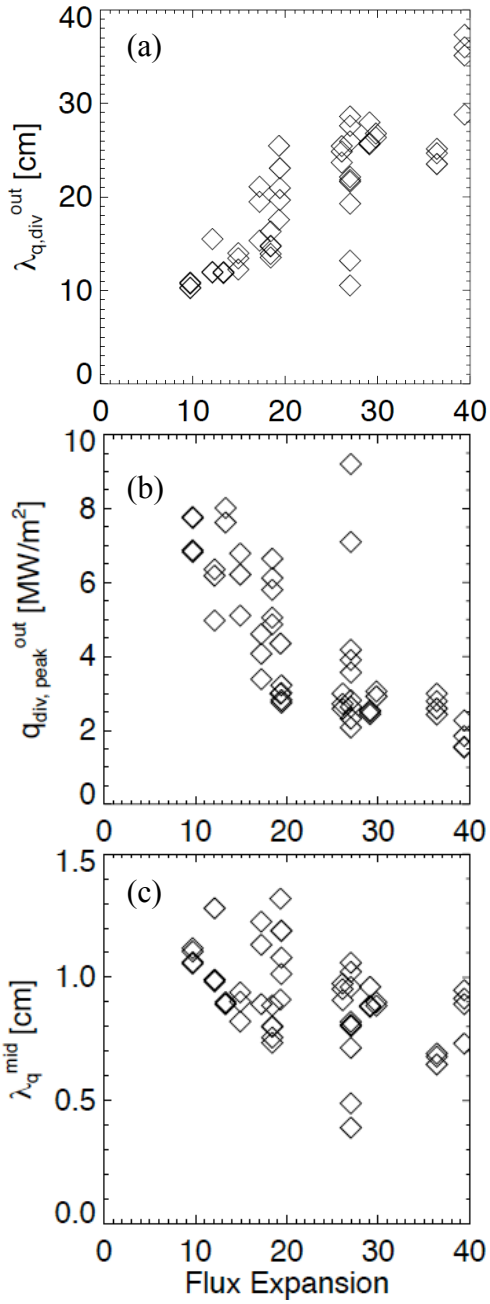

Fig. 6: dependence of divertor and (mapped) midplane heat flux widths on divertor magnetic flux expansion.

<u>NSTX research</u> (R. Maingi, V. Soukhanovskii)

Preparation for operation in NSTX with the newly installed liquid lithium divertor (LLD) tray continues, with first plasma expected early in 3QFY10. Thus, much of the activity in the quarter has focused on refinement of the analysis of the dependence of heat flux widths on flux expansion, heating power, and plasma current, which were presented to the members of the NSTX Program Advisory Committee. These results will be documented in an article at the 2010 PSI conference[4].

A wide scan in the divertor flux expansion was accomplished in past NSTX experiments by variation of the X-point height[5]. The goal here is

to evaluate the dependence of the divertor and midplane heat flux footprint widths on flux expansion. It was found that the outer divertor heat flux profile width, $\lambda_{q,div}^{out}$, scaled nearly linearly with flux expansion over a wide range (Fig. 6a). Here $\lambda_{q,div}^{out} = P_{div}^{out}/(2\pi r_{div}^{out} \times q_{div,peak}^{out})$, where

P_{div}^{out} = total power incident on outer div.

r_{div}^{out} = radius of peak heat flux

$q_{div,peak}^{out}$ = outer divertor peak heat flux

Consequently, the $q_{div,peak}^{out}$ decreased inversely with flux expansion such that the total power incident on the outer divertor was approximately constant. The divertor width $\lambda_{q,div}^{out}$ can be related[6] to an equivalent midplane heat flux width with magnetic mapping, assuming that the widths do not change substantially: $\lambda_q^{mid} = \lambda_{q,div}^{out} / f_{exp}$

where f_{exp} is the magnetic flux expansion:

$f_{exp} = r_{mid} B_\theta^{mid} / (r_{div}^{out} B_\theta^{div})$

$r_{mid} = r_{div}^{out}$ mapped to the midplane

B_θ^{mid} = midplane poloidal field strength

B_θ^{mid} = divertor poloidal field strength

Figure 6c confirms that the equivalent midplane-mapped heat flux footprint depends only weakly on magnetic flux expansion, if at all.

A refined analysis shows that λ_q^{mid} is relatively independent of power flowing into the SOL when the divertor is in the "attached" state, i.e. with relatively low radiated power and momentum loss. Figure 7a, 7b illustrate these points from a set of discharges at intermediate δ=0.5 and I_p=0.8 MA: at $P_{loss} \simeq 4$ MW, there is a clear transition to a narrow footprint in terms of λ_q^{mid}. For higher P_{loss}, the λ_q^{mid} appears insensitive with a range between 1.0-1.8 cm. Figure 7c, 7d plot the dependences over the P_{loss}, range 4-7 MW, with data from a sequence of high δ=0.7 and I_p=1.2 MA discharges. The relative insensitivity of λ_q^{mid} to P_{loss} is also apparent in those data, as is the reduction of λ_q^{mid} at high I_p.

Using the results shown in figures 6 and 7 that the λ_q^{mid} is relatively insensitive to P_{loss} (for high P_{loss}) and flux expansion, data from different δ and f_{exp} are combined to quantify the dependence of $q_{div,peak}^{out}$ and λ_q^{mid} on I_p in Figure 8. All discharges had fixed

B_t=0.45 T. In NSTX the λ_q^{mid} decreases faster than inversely with I_p, consistent with past

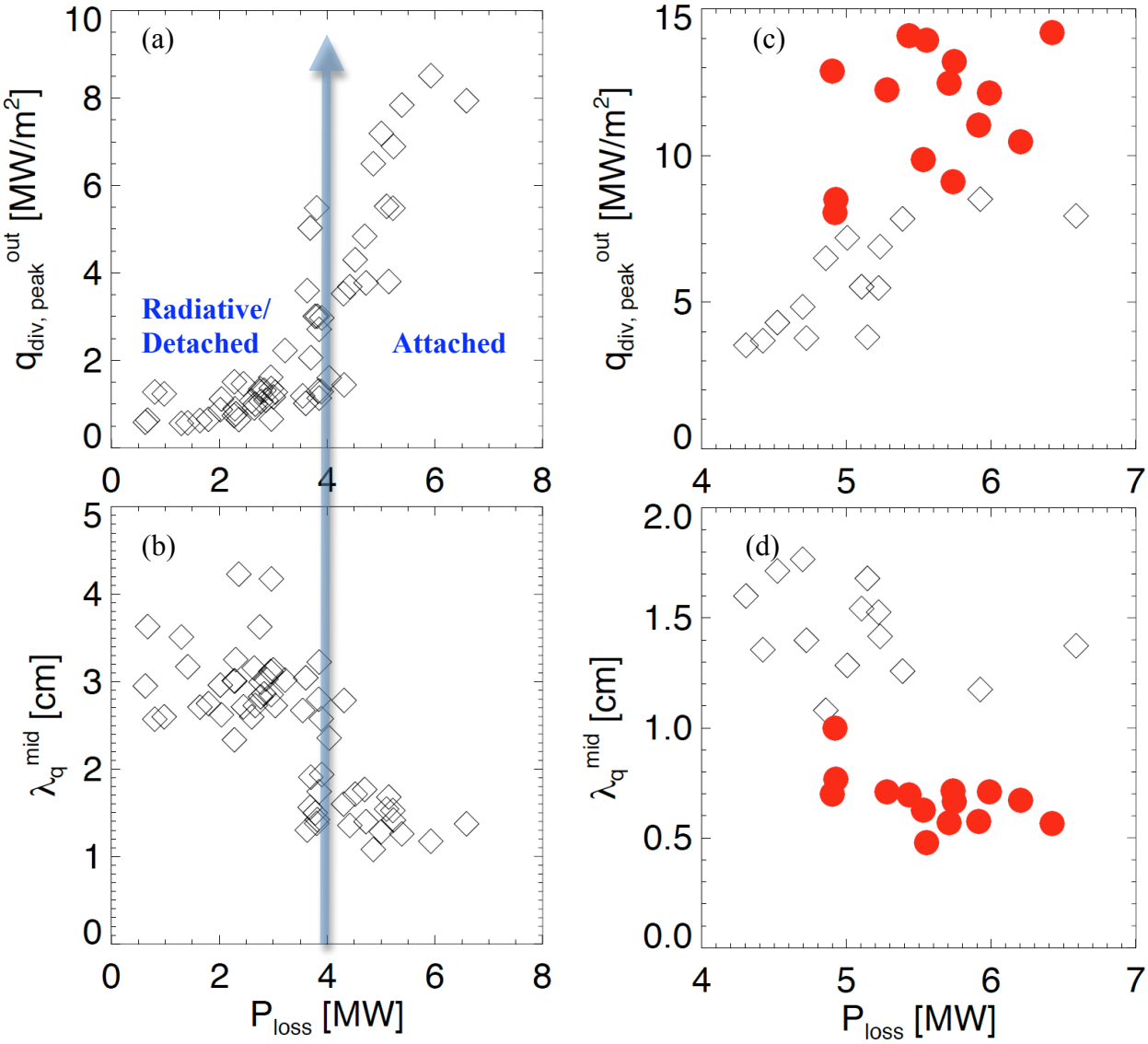

Fig. 7: dependence of peak outer divertor heat flux and midplane-equivalent widths on power flow into the SOL, P_{loss}. The black diamonds were obtained at intermediate triangularity $\delta \sim 0.5$ and I_p =0.8 MA, whereas the red circles were obtained at high $\delta \sim 0.7$ and I_p =1.2 MA.

results[7]; in comparison, DIII-D[8] and JET[9] have reported an inverse proportionality in the past. The extent to which this dependence is a q_{95} or connection length dependence, as compared with a direct I_p dependence, will be documented in the coming experiments this year.

In addition, diagnostic and analysis upgrades were continued in preparation for operation with the recently installed LLD. Specifically the recently installed[10] fast-time response IR camera has been retro-fitted to split the output into two color bands[11]. An upgrade is necessary because the existing IR cameras require an absolute calibration, which is related to the emissivity of the target. While the underlying graphite is a blackened, highly emissive surface (emissivity ~ 0.9), the variable lithium coating is highly reflective (emissivity < 0.2), leading to uncertainty in the absolute heat flux in discharges with lithium wall conditioning (all of the data in figures 1-3 were obtained before lithium application for that run campaign). In theory, the emissivity of the lithium surface should affect the IR emission in each of those bands equally, such that the ratio of the intensities in those two bands should be insensitive to the variation in emissivity caused by the presence of lithium. Advanced testing of the retro-fitted camera is in progress, with the goal of obtaining data from the beginning of the FY10 run campaign. Specifically additional data on the B_t and δ_r^{sep} dependence will be obtained, as well as data at even higher I_p and low collisionality.

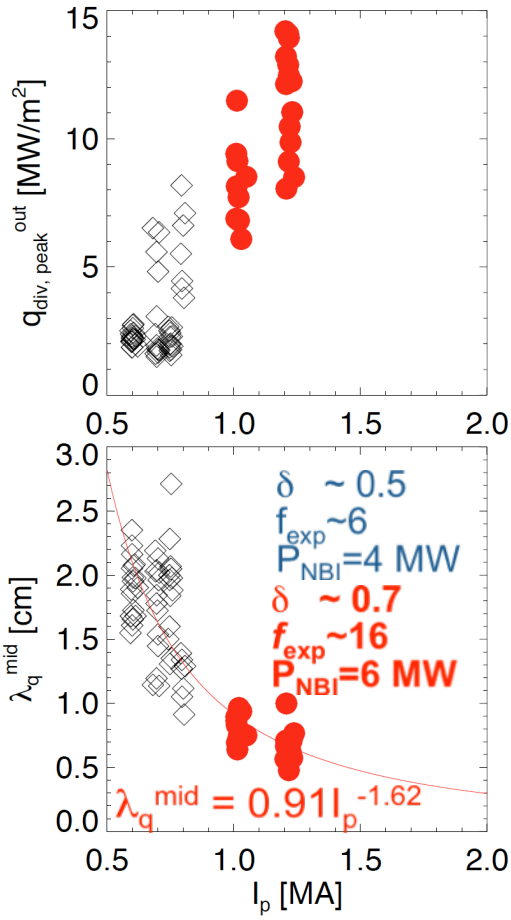

Fig. 8: dependence of peak outer divertor heat flux and midplane-widths on plasma current, I_p.

Finally analysis of divertor characteristics with an innovative divertor configuration, i.e. the "snowflake divertor" (SFD)[12], represents part of NSTX's contribution to this milestone from the perspective of improved heat flux handling. This magnetic topology was recently realized in NSTX, resulting in divertor peak heat flux reduction and impurity control. In this case, the divertor heat flux footprint is broadened by easing the access to partial detachment, which leads to a substantial increase in the midplane-equivalent footprint. These initial results will be documented in an upcoming article[13].

In recent NSTX experiments with the SFD configuration, a reduction in peak divertor heat flux due to a partially detached strike point region, and a significant reduction in core carbon density and radiated power were observed, in 0.8 MA 4-6 MW NBI-heated H-mode discharges. These initial experiments confirmed the attractive SFD properties predicted by analytic theory[12] and two-dimensional multi-fluid numerical modeling[14]. The SFD concept uses a second-order X-point created by merging, or bringing close to each other, two first-order X-points of a standard divertor configuration. The possibility of forming the SFD configuration has been demonstrated through magnetic equilibria modeling for DIII-D and NSTX, and in experiments on TCV[15]. The SFD-like configuration was generated in NSTX using two divertor magnetic coils controlled in real time by the plasma control system. When compared to the high-triangularity (δ=0.7-0.8) standard divertor configuration in NSTX[16], the obtained SFD configuration with a medium triangularity (δ=0.5-0.65) had a connection length $l_{||}$ longer by factors of 1.5-2, and a divertor poloidal flux expansion f_{exp} higher by factors of 2-3. Divertor heat flux profiles showed low relative heat flux in the greatly expanded region near the outer divertor strike point during the SFD periods (Fig. 9). Divertor radiation due to carbon impurity was significantly increased in the SFD. As inferred from the spatially-resolved ultraviolet spectroscopy measurements and collisional-radiative and Stark spectral line broadening modeling, a volume recombination region with T_e ~ 1.5 eV, n_e > 3 x 10^{20} m^{-3} developed in the X-point and strike point regions, suggesting an increase in volumetric momentum losses in the divertor and a partial detachment of the first several mm of the scrape-off layer (SOL) width (as mapped to the midplane). Importantly, the SFD

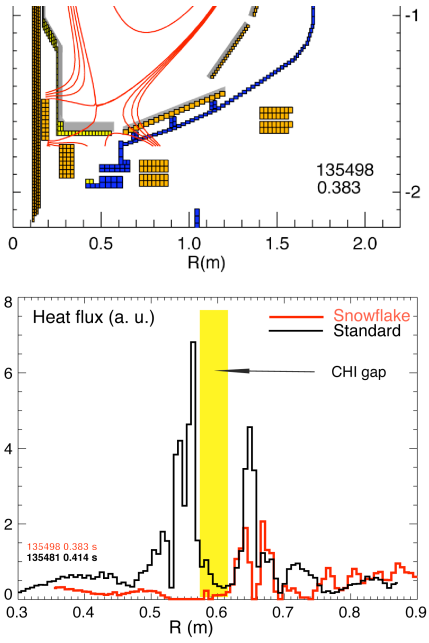

Fig. 9. (Top) The "snowflake" divertor configuration obtained in NSTX with 3 mm SOL flux surfaces shown; (bottom) Divertor heat flux profiles measured by IR camera in discharges with a standard medium δ divertor and with the "snowflake" divertor configurations

partial detachment was obtained in reduced density discharges with lithium conditioning, in contrast to previous NSTX divertor detachment experiments that required an additional divertor gas injection[16]. The core carbon density was reduced by up to 50 % in the SFD discharges, with little degradation of H-mode stored energy and confinement. Looking ahead, documentation of the power loss mechanisms from the midplane to the divertor in light of the enhanced divertor radiating volume due to the SFD topology is a high priority in the coming FY2010 experiments.

References

[1] B. LaBombard, et. al., *J. Nucl. Mater.* (2010) to be submitted.
[2] D. Brunner, et. al., *J. Nucl. Mater.* (2010) to be submitted.
[3] J. L. Terry, et. al., *Rev. Sci. Instrum.* (2010) to be submitted.
[4] R. Maingi, et. al., *J. Nucl. Mater.* (2010) to be submitted.
[5] V. A. Soukhanovskii, et. al., *Proc. 36th EPS Conf. on Plasma Physics, Europhys. Conf. Abs.* (2009) P2.178.
[6] A. Loarte, et. al., *J. Nucl. Mater.* **266-269** (1999) 587.
[7] R. Maingi, et. al., *J. Nucl. Materials* **363-365** (2007) 196.
[8] C. J. Lasnier, et. al., *Nuclear Fusion* **38** (1998) 1225.
[9] W. Fundamenski, et. al., *Private Comm.* (2010).
[10] J. W. Ahn, et. al., *Rev. Sci. Instrum.* **81** (2010) 023501.
[11] A. G. McLean, et. al., *Rev. Sci. Instrum.* (2010) submitted.
[12] D. D. Ryutov, et. al., *Phys. Plasma* **14** (2007) 064502.
[13] V. A. Soukhanovskii, et. al., *Phys. Rev. Lett.* (2010) to be submitted.
[14] M. V. Umansky, et. al., *Nucl. Fusion* **49** (2009) 075005.
[15] F. Piras, et. al., *Plasma Phys. Contr. Fusion* **16** (2009) 055009.
[16] V. A. Soukhanovskii, et. al., *Nucl. Fusion* **49** (2009) 095025.